OPEN ACCESS Freely available online

PLoS one

Modulation by Endothelin-1 of Spontaneous Activity and Membrane Currents of Atrioventricular Node Myocytes from the Rabbit Heart

Stéphanie C. Choisy[1], Hongwei Cheng[1], Godfrey L. Smith[2], Andrew F. James[1]*, Jules C. Hancox[1]*

1 School of Physiology & Pharmacology, Medical Sciences Building, University of Bristol, Bristol, United Kingdom, **2** Cardiovascular Physiology, University of Glasgow, Glasgow, United Kingdom

Abstract

Background: The atrioventricular node (AVN) is a key component of the cardiac pacemaker-conduction system. Although it is known that receptors for the peptide hormone endothelin-1 (ET-1) are expressed in the AVN, there is very little information available on the modulatory effects of ET-1 on AVN electrophysiology. This study characterises for the first time acute modulatory effects of ET-1 on AVN cellular electrophysiology.

Methods: Electrophysiological experiments were conducted in which recordings were made from rabbit isolated AVN cells at 35–37°C using the whole-cell patch clamp recording technique.

Results: Application of ET-1 (10 nM) to spontaneously active AVN cells led rapidly (within ~13 s) to membrane potential hyperpolarisation and cessation of spontaneous action potentials (APs). This effect was prevented by pre-application of the ET_A receptor inhibitor BQ-123 (1 μM) and was not mimicked by the ET_B receptor agonist IRL-1620 (300 nM). In whole-cell voltage-clamp experiments, ET-1 partially inhibited L-type calcium current ($I_{Ca,L}$) and rapid delayed rectifier K^+ current (I_{Kr}), whilst it transiently activated the hyperpolarisation-activated current (I_f) at voltages negative to the pacemaking range, and activated an inwardly rectifying current that was inhibited by both tertiapin-Q (300 nM) and Ba^{2+} ions (2 mM); each of these effects was sensitive to ET_A receptor inhibition. In cells exposed to tertiapin-Q, ET-1 application did not produce membrane potential hyperpolarisation or immediate cessation of spontaneous activity; instead, there was a progressive decline in AP amplitude and depolarisation of maximum diastolic potential.

Conclusions: Acutely applied ET-1 exerts a direct modulatory effect on AVN cell electrophysiology. The dominant effect of ET-1 in this study was activation of a tertiapin-Q sensitive inwardly rectifying K^+ current via ET_A receptors, which led rapidly to cell quiescence.

Citation: Choisy SC, Cheng H, Smith GL, James AF, Hancox JC (2012) Modulation by Endothelin-1 of Spontaneous Activity and Membrane Currents of Atrioventricular Node Myocytes from the Rabbit Heart. PLoS ONE 7(3): e33448. doi:10.1371/journal.pone.0033448

Editor: Marcello Rota, Brigham & Women's Hospital - Harvard Medical School, United States of America

Received November 7, 2011; **Accepted** February 10, 2012; **Published** March 29, 2012

Funding: This work was funded by a project grant from the British Heart Foundation (PG/08/104). The funders had no role in study design, data collection and analysis, decision to publish, or preparation of the manuscript.

Competing Interests: The authors have declared that no competing interests exist.

* E-mail: jules.hancox@bristol.ac.uk (JCH); a.james@bristol.ac.uk (AFJ)

Introduction

The atrioventricular node (AVN) is a small yet critically important component of the cardiac pacemaker-conduction system that lies at the junction between right atrium and ventricle [1,2]. It is normally the only site where electrical activity can pass from atria to ventricles [1,2]. Comparatively slow conduction through the AVN co-ordinates the normal timing of atrial then ventricular excitation [2,3] and in the setting of supraventricular tachycardias such as atrial fibrillation, this limits impulse transmission to the ventricles [2,4]. On the other hand, aberrant AVN conduction can itself lead to arrhythmia [2,5]. The AVN also has pacemaking properties [2,5]. Normally these are subordinate to the heart's dominant pacemaker the sinoatrial node (SAN); however, should the SAN fail the AVN can take over pacemaking of the ventricles [2,5]. AVN pacemaking is incompletely understood, but is established to involve an interplay between the activity of a number of different ionic conductances [6–10].

Endothelin-1 (ET-1) is a potent vasoactive peptide hormone that is produced constitutively within the heart by vascular and endocardial endothelial cells. There is also evidence for ET-1 release by cardiac myocytes [11,12]. In addition to its vasoconstrictor action, endogenous release of the hormone is known to modulate the inotropic state of the heart and is also suggested to play a role in modulation of the heart rate (e.g. [13–16]). Elevated production and release of ET-1 is strongly implicated in the pathogenesis of heart failure and the generation of arrhythmias (for reviews see [17–19]). There is also evidence that ET-1 can be pro-arrhythmic independent of coronary vasoconstriction [12,19]. Data from patients with angina pectoris have shown left bundle-branch block to be associated with raised ET-1 levels, suggesting that the hormone may be involved in conduction abnormalities [20]. Consistent with an ability of ET-1 to exert a direct effect on the pacemaker-conduction system, experiments on cells isolated from the rabbit SAN have demonstrated that ET-1 produces a

negative chronotropic effect that is associated with direct ion channel modulation [21–23]. By contrast, to our knowledge, there is no current information available concerning direct effects of this peptide hormone on the AVN. Autoradiographic studies of the human myocardium have revealed a high density of ^{125}I-ET-1 binding to the AVN and the penetrating and branching bundles of His, in addition to the atrial and ventricular myocardium [24]. Autoradiographic study of the porcine AVN has also demonstrated the presence of specific ^{125}I-ET-1 binding sites in this region [25]. Indirect evidence that ET-1 can modulate AVN electrophysiology comes from electrocardiogram measurements from anaesthetised dogs and rats, which have shown that intra-coronary ET-1 administration can produce complete AV block [26,27]. Although, when considered together, the effect of intra-coronary ET-1 and evidence for presence of ET receptors in the AVN are strongly suggestive of a direct action of ET-1 on AVN electrophysiology, they are not conclusive in this regard. The present study was therefore undertaken to address this gap in information, by using an established rabbit single AVN cell preparation [6,28–32]. The study was conducted to establish the effects of ET-1 on: (i) AVN cell spontaneous activity and (ii) major ionic currents present in AVN. The results that emerge demonstrate that ET-1 exerts marked direct effects on AVN cell electrophysiology and also implicate endothelin-A (ET_A) receptors in the observed modulatory actions.

Materials and Methods

Ethics statement

All procedures used in these experiments were approved by the University of Bristol ethics committee and adhere to the United Kingdom Home Office Animals Scientific Procedures Act of 1986.

Rabbit AVN cell isolation

Male New-Zealand White rabbits (~2.0 to 3.5 kg) were killed in accord with UK Home Office legislation, their hearts then rapidly excised and cells isolated from the entire atrioventricular nodal (AVN) region using an established enzymatic and mechanical dispersion technique [28,29;33]. Isolated AVN cells were suspended in Kraft-Brühe "KB" solution [28,34] and stored in a refrigerator until use.

Electrophysiological recording

For recording, cells were transferred in KB solution into an experimental chamber (0.5 ml) mounted on the stage of an inverted microscope (Nikon Diaphot) and left to settle for 10 mins prior to superfusion with a normal Tyrode's solution, containing (in mM): NaCl 140, KCl 4, $CaCl_2$ 2, $MgCl_2$ 1, HEPES 5 and Glucose 10, (pH 7.4 with NaOH). ET-1 and other compounds were added to this solution. Patch-pipettes (Corning 7052 glass, AM Systems Inc, Sequim, WA, USA) were pulled using a P-97 Flaming/Brown micropipette puller (Sutter Instruments, Novato, CA, USA) and filled with a solution containing (in mM) [10;33]: KCl 110, NaCl 10, HEPES 10, $MgCl_2$ 0.4, and Glucose 5, K_2ATP dihydrate 5, GTP-Tris salt 0.5 (pH 7.1 with KOH). For ionic current but not action potential measurements the pipette solution also contained 5 mM BAPTA (*cf* [10,33]). Recordings were made using an Axopatch 1D amplifier (Axon Instruments; now Molecular Devices, Sunnyvale, CA, USA). Pipette resistance was typically <3 MΩ; series resistance values were usually <7 MΩ (mean of 6.07 ± 0.68 MΩ; $n=23$) and ~60–80% of the series resistance was compensated. Membrane capacitance values used for calculation of current densities (pA/pF) were obtained and compensated for using capacitance compensation on the recording amplifier; cell capacitance values obtained in this way have been shown previously to match closely those obtained using a 'surge' technique [28]. For voltage clamp experiments, membrane potential was held at -40 mV (as this corresponds to the zero current potential for rabbit AVN cells [28,30]). Action potentials were recorded from spontaneously beating cells in current-clamp mode with zero-current injection, using a gap-free

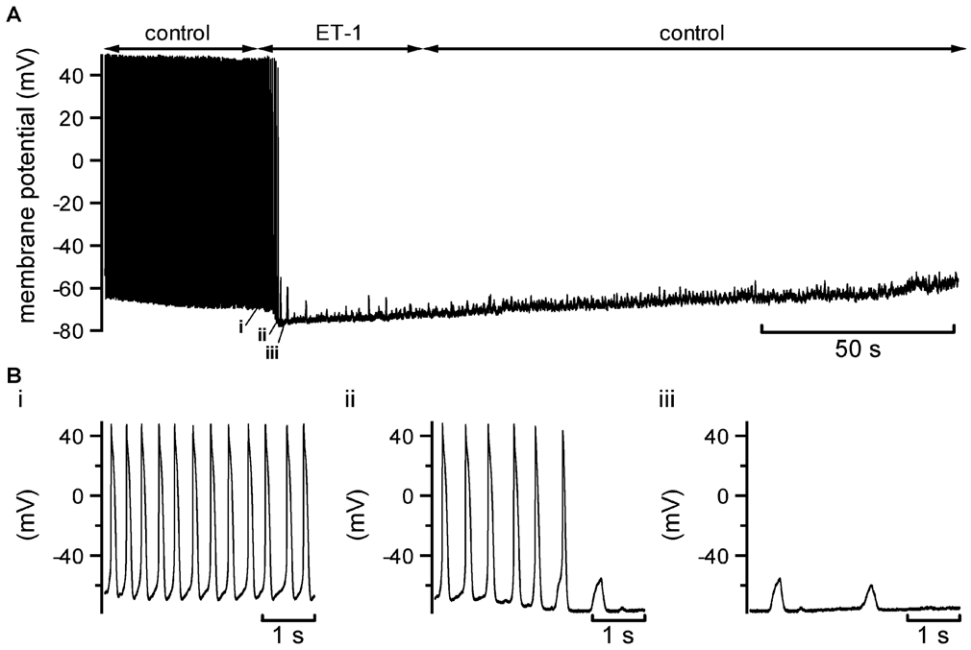

Figure 1. Effects of ET-1 on spontaneous APs. A. Slow time-base recording of APs before, during and after rapid application of 10 nM ET-1. B. Expanded (faster time-base) portions of the recording extracted from numbered sections of panel A (indicated labels i, ii, iii). Similar results were observed in 9 experiments.
doi:10.1371/journal.pone.0033448.g001

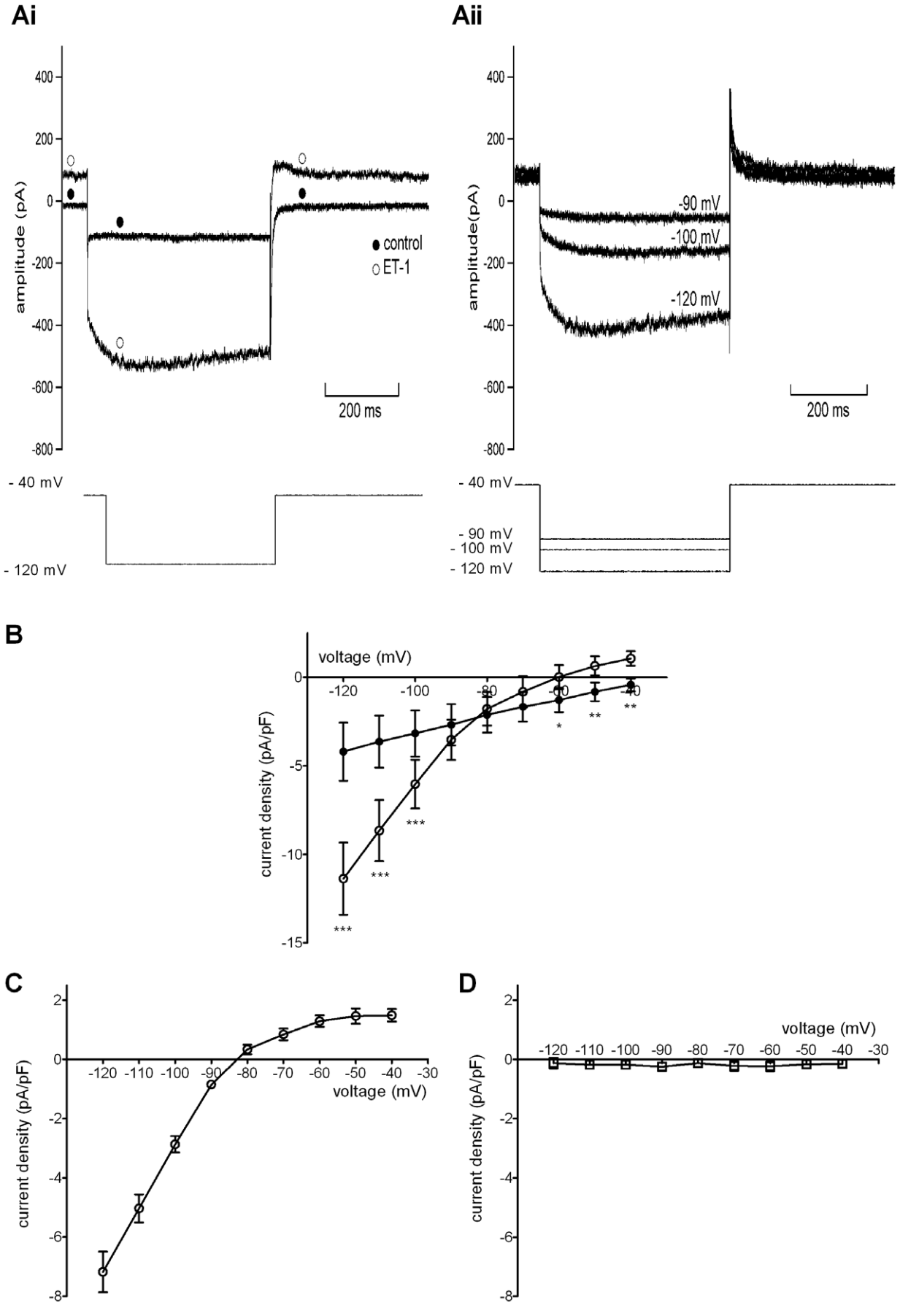
Ai
Aii
amplitude (pA)
control
ET-1
200 ms
- 40 mV
- 120 mV
amplitude(pA)
-90 mV
-100 mV
-120 mV
- 90 mV
- 100 mV
B
voltage (mV)
current density (pA/pF)
C
D
voltage (mV)

Figure 2. Modulation by ET-1 of instantaneous current in cells lacking I_f. Ai. Currents recorded in the absence (control) and the presence of 10 nM ET at −120 mV (upper traces) when a voltage command was applied from −40 mV for 500 ms (lower trace). Note outward shift in holding current with ET-1. Closed circles indicate control trace; open circles indicate trace in ET-1. Aii. ET-1 activated currents (elicited at −90, −100 and −120 mV) obtained by digital subtraction of control from ET-1 records (same cell as Ai). B. Mean current-voltage (I–V) relationships for current measured at the start of applied voltage commands in absence (control, filled circles) and presence (open circles) of 10 nM ET-1 (n = 7). Asterisks denote statistical significance ($p<0.05$ *, $p<0.01$ **, $p<0.001$ ***). C. Plot of the mean I–V relationship for ET-1 sensitive difference (ET-1 activated) calculated from the same cells shown in B. D. Plot of ET-1 sensitive current when ET-1 was applied after 1 μM BQ-123 (n = 4).
doi:10.1371/journal.pone.0033448.g002

acquisition mode. Protocols were generated and data recorded using Clampex 8 (Axon Instruments; now Molecular Devices Sunnyvale, CA, USA). Data digitization rates were 10–25 kHz with an appropriate bandwidth of 2–10 kHz set on the amplifier.

Solutions and Chemicals

Cells were superfused with experimental solutions at 35–37°C (checked regularly using a hand-held thermocouple). ET-1 and other compounds were applied externally to the cell under study using a home-built, rapid solution exchange device capable of exchanging superfusate in <1 s [35]. ET-1 (Sigma-Aldrich Company Ltd, Dorset, UK) was used at 10 nM from a stock solution of 100 μM prepared in 0.1% acetic acid. This concentration falls within the range of ET-1 concentrations used in prior cardiomyocyte studies (1–100 nM; e.g. [21,23,36]). The selective ET_A receptor antagonist BQ-123 (Sigma-Aldrich Company Ltd, Dorset, UK) was used at a maximally effective concentration of 1 μM [37] from a 1 mM stock solution made in deionised water, whilst the endothelin-B receptor (ET_B) selective agonist IRL-1620 (Tocris Bioscience, Bristol, UK) [38] was superfused at a concentration of 300 nM from a 1 mM stock solution prepared in 0.1% acetic acid. Tertiapin-Q (Tocris Bioscience, Bristol, UK) and barium ions (Ba^{2+}, as $BaCl_2$, (Sigma-Aldrich Company Ltd, Dorset, UK)) were prepared in deionised water and respectively used at 300 nM and 2 mM. All drugs were aliquoted and stored at −20°C, except $BaCl_2$ solution, which was stored at 4°C.

Data analysis

Data were analysed and graphical plots produced using Clampfit 10.2 software (Molecular Devices Sunnyvale, CA, USA), Microsoft Excel (2003), GraphPad Prism (v5; GraphPad Software Inc, La Jolla, CA, USA), IgorPro (v3.16B, Wavemetrics Inc, Portland, OR, USA) and SigmaPlot (v12; Systat Software Inc, Chicago, IL, USA). Data are presented as mean ± standard error of the mean (SEM). Statistical analysis was performed using Student's *t*-test or two-way ANOVA with Bonferroni or Tukey post-hoc tests, as appropriate. Values of 'p' less than 0.05 were taken as significant.

Current-voltage relations for L-type Ca current ($I_{Ca,L}$) and rapid delayed rectifier current (I_{Kr}) were fitted with following equations:

$$I_{Ca,L} = [G_{\max}(V_m - V_{rev})]/[1 + \exp((V_{0.5} - V_m)/k)] \qquad (1)$$

where G_{max} is maximal $I_{Ca,L}$ conductance, V_m is the test potential at which $I_{Ca,L}$ was measured, V_{rev} is the reversal potential determined from extrapolation of the ascending limb of plotted current-voltage relations, $V_{0.5}$ is the potential at which $I_{Ca,L}$ activation is half maximal and k is the slope factor describing current activation.

$$I_{tail} = I_{tail(Max)}/(1 + \exp[(V_{0.5} - V_m)/k]) \qquad (2)$$

where I_{tail} represents I_{Kr} tail current amplitude recorded at −40 mV following a given test pulse membrane potential (V_m) and $V_{0.5}$ and k have similar meanings to those for equation 1.

Results

Effects of ET-1 application on spontaneous APs

Spontaneous APs were measured in whole-cell membrane potential recording mode from cells selected on the basis of exhibiting regular spontaneous activity (evidenced visually as regular spontaneous cell beating) during superfusion of control Tyrode's solution. Figure 1A shows a representative slow time-base record of APs, before, during and following exposure to 10 nM ET-1, whilst Figures 1Bi–iii show faster time-base extracts at the time-points indicated on Figure 1A. The mean spontaneous AP rate in control solution was 3.47±0.35 AP s^{-1} (n = 9), compatible with rates seen in previous studies [10,28,31,33]). Application of ET-1 led rapidly to membrane potential hyperpolarisation and to cessation of spontaneous APs (within 13.1±2.1 s of ET-1 application; n = 9). As shown in Figure 1A, after reaching an initial peak response (the mean peak membrane potential hyperpolarisation produced by ET-1 in comparison to control maximum diastolic potential values was −20.3±2.0 mV, n = 9), membrane potential showed gradual depolarisation but without a return of spontaneous activity. As has been reported in some other studies (e.g. [21,39]), the effect of ET-1 was not reversible on washout and membrane potential continued to show modest membrane potential depolarisation throughout the remainder of the measurement period. In all cells, whilst on ET-1 application cells rapidly ceased to generate spontaneous APs, small membrane potential oscillations were visible (of mean amplitude 3.5±0.3 mV, n = 9 cells; more than 25 oscillations analysed per cell), with occasional oscillations exceeding 10 mV; see Figures 1A and 1Bii and iii).

Effects of ET-1 on ionic currents at negative membrane potentials

AVN cell sub-types exhibiting time-independent and time-dependent current (I_f) on membrane potential hyperpolarisation in standard extracellular solution have been identified [29,31]. The effects of ET-1 were determined on cells with both response types. Effects of ET-1 were determined by application of 500 ms duration hyperpolarising voltage clamp commands: from a holding potential of −40 mV membrane potential was stepped to more negative potentials between −120 and −40 mV in 10 mV increments (at a pulse frequency of 0.2 Hz). Figure 2Ai shows current records elicited on membrane potential hyperpolarisation to −120 mV, for a cell that exhibited only time-independent current in control solution. On the application of ET-1, holding current shifted outwards (in control, holding current at −40 mV was −0.4±0.3 pA/pF, n = 7, NSD from zero current; in ET-1 this became 1.1±0.4 pA/pF; $p<0.001$ versus control). At −120 mV a large inward current was induced, with a marked increase in instantaneous inward current. Some time-dependence of the current can be seen in this example. Figure 2Aii shows ET-1 sensitive (activated) current from the same cell, at −90, −100 and −120 mV. Outward holding current is visible prior to the marked inward current elicited on membrane potential hyperpolarisation, the amplitude of which increased progressively with the magnitude

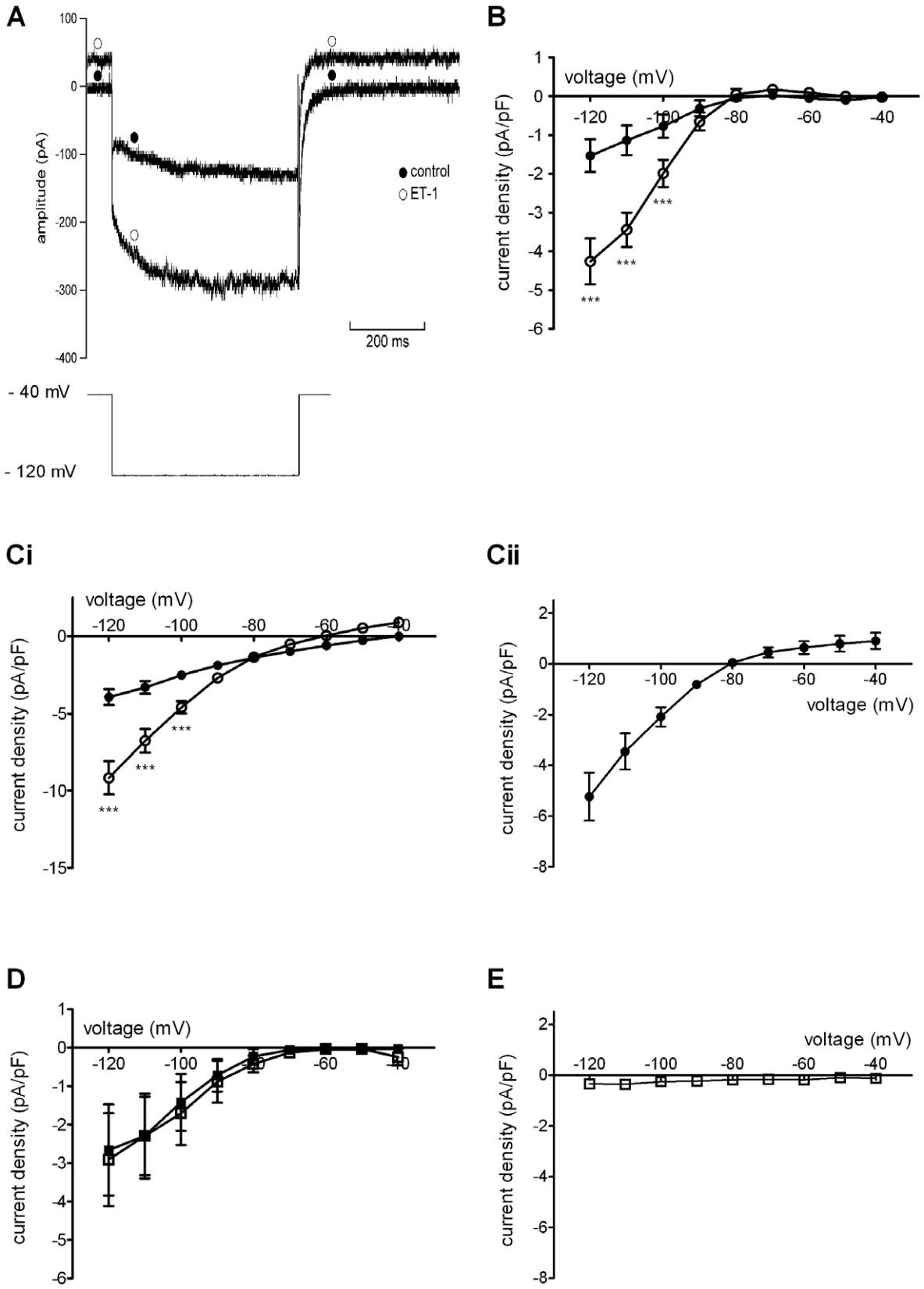

Figure 3. ET-1 effects on the hyperpolarisation-activated current I_f. A. Upper traces show currents elicited −120 mV in an I_f-expressing cell in control solution and 10 nM ET-1 by protocol shown in bottom trace. Note outward shift in holding current in presence of ET-1. Closed circles indicate control trace; open circles indicate trace in ET-1. B. Mean I–V relationships (n = 7) for I_f, plotted as time-dependent current during command pulses, in absence (control, filled circles) and presence of 10 nM ET-1 (open circles). The activating effect of ET-1 was significant only at −120, −110

and −100 mV. C. Mean I–V relationships for the instantaneous current recorded at the beginning of the test-pulse (Ci: in absence (control, filled circles) and presence (open circles) of 10 nM ET-1). Cii shows I–V relation for the ET-1 activated instantaneous current (Cii, filled circles), in cells also showing I_f (n = 7). ET-1 activates a large inwardly rectifying current. D. I–V relations for I_f in presence of 1 μM BQ-123 (n = 11) without (filled squares) and with 10 nM ET-1 (open squares, n = 11 at all potentials except at −50 mV, where n = 10). BQ-123 prevented stimulation of I_f by ET-1. E. Inhibitory effect of 1 μM BQ-123 on the ET-1 activated current in cells exhibiting showing I_f (open squares, n = 12 except at −50 mV where n = 11). Asterisks denote statistical significance ($p<0.001$ ***).
doi:10.1371/journal.pone.0033448.g003

of the applied hyperpolarising step. The stimulatory effect of ET-1 in augmenting time-independent (instantaneous) current was quantified by plotting current density-voltage relations for instantaneous current in control and in ET-1 (Figure 2B) and also by deriving from individual experiments the ET-1 sensitive difference (ET-1 activated) current, the mean of which is plotted in Figure 2C. Net instantaneous current (Figure 2B) was augmented by ET-1 across a range of potentials, with a left-ward shifted zero-current potential compared to control; control and ET-1 current-voltage relations intersected near −80 mV (Figure 2B). The ET-1 activated current (Figure 2C) showed marked inward rectification and reversed at ~−82 mV (with a mean reversal potential derived from individual cell data of −82.1±1.2 mV; n = 7). The activation of this current accounts for the left-ward shift in zero current potential for net instantaneous current visible in Figure 2B. The ET-1 activated current was outwardly directed over potentials relevant to the diastolic potential range (typically between −65 and −40 mV). The ET-1 response showed some time-dependent 'fade' in the continued presence of the peptide: the mean amplitude of the ET-1 activated current at −120 mV immediately following (within 10–20 s) of ET-1 application was −7.2±0.7 pA/pF (n = 7), whilst at ~2 minutes following ET-1 this had declined to −1.7±0.3 pA/pF (n = 7; $p<0.001$ versus immediate response) and in two cells that lasted ~3.5 minutes following ET-1 this was −0.6±0.2 pA/pF. In cells pre-treated with BQ-123, ET-1 did not activate such a current: Figure 2D shows the instantaneous ET-1 sensitive difference current in cells exposed to BQ-123 prior to ET-1 application. This implicates ET_A receptor activation in the observed response.

Figure 3 shows comparable data for cells that exhibited I_f in control. Figure 3A shows representative currents in control solution and in the presence of ET-1. A dual effect was seen, in which both instantaneous and time-dependent current components were augmented in the presence of ET-1. Previously, I_f from AVN cells has been measured as the difference between end-pulse current and instantaneous current observed at the start of the hyperpolarising step [29,33] and this method was used here to produce the mean I–V relations shown in Figure 3B. As reported previously [29,33], under these conditions there was little I_f between −60 and −80 mV in control Tyrode's solution, whilst significant I_f was evident at more negative voltages. In the presence of ET-1, time-dependent current was significantly augmented at potentials of −100 mV and more negative than this (Figure 3B). However, this response was transient: the mean amplitude of I_f at −120 mV immediately following (within 10–20 s) of ET-1 was −4.3±0.6 pA/pF (n = 7), whilst at ~2 minutes following ET-1 this was −1.9±0.7 pA/pF (n = 7; $p<0.001$ versus the immediate response), with the current at ~3.5 minutes following ET-1 similar to that following 2 minutes of exposure. Figures 3Ci and Cii show effects of ET-1 on the instantaneous current component (i.e. comparable data to those shown in Figures 2B and 2C), demonstrating that activation of an inwardly rectifying instantaneous current also occurred in these cells. Figure 3Ci shows mean net instantaneous current in control and ET-1, again showing a left-ward shift in zero-current potential and intersection of the two relations close to −80 mV. Figure 3Cii shows the current-density plot for ET-1 activated current, which resembles that in Figure 2C. Note that the magnitude of the ET-1 activated current was not significantly different from that from cells that lacked I_f, except at −120 mV ($p<0.01$ at this potential only). Figure 3D shows plots of time-dependent I_f in the presence of BQ-123 and BQ-123+ET-1. These were closely superimposed, implicating ET_A receptors in the effect of ET-1 on I_f. Figure 3E shows that, similar to cells lacking I_f (Figure 2), ET-1 failed to activate instantaneous inwardly rectifying current in the presence of BQ-123.

Effects of ET-1 on $I_{Ca,L}$

Similar to other recent studies from our laboratories [10,33], the effects of ET-1 on $I_{Ca,L}$ were determined from currents measured over a range of test potentials (500 ms commands were applied to voltages between −30 and +50 mV from a holding potential of −40 mV). Figure 4A shows representative traces of $I_{Ca,L}$ elicited by depolarisation from −40 mV to +10 mV in the absence and presence of ET-1, showing a marked suppression of peak current amplitude by ET-1. Figure 4B shows mean current-voltage relations for $I_{Ca,L}$ in control and with ET-1. Repeated applications of the $I_{Ca,L}$ measurement protocol in the presence of ET-1 did not lead to significant further reductions in current beyond that shown in Figure 4A. A fit to the data with equation 1 yielded an activation $V_{0.5}$ of −2.7±0.6 mV in control and of −1.0±1.9 mV in ET-1 (n = 11 cells; $p>0.1$), whilst G_{max} values derived from the fits to the data were 0.36±0.03 nS/pF (control) and 0.16±0.03 nS/pF (ET-1; $p<0.001$). In 12 further experiments, cells were exposed to the ET_A receptor antagonist BQ-123 (1 μM) prior to ET-1 application. Figure 4C shows mean I–V relations from these experiments: with BQ-123 application prior to ET-1 superfusion, ET-1 did not reduce $I_{Ca,L}$ amplitude at any membrane voltage, implicating ET_A receptor activation in this action of ET-1. In 6 cells in which $I_{Ca,L}$ at +20 mV was monitored during ET-1 exposure and following washout, the inhibitory effect of ET-1 was not reversed by washout.

Effects of ET-1 on rapid delayed rectifier K^+ current, I_{Kr}

The rapid delayed rectifier K^+ current, I_{Kr}, is important to AVN AP repolarisation and can also influence spontaneous rate [33,40–42]. I_{Kr} is typically measured from AVN cells as outward tail current on repolarisation to a negative voltage following depolarising voltage commands, and lacks contamination from potentially overlapping currents such as I_{Ks}, which is absent from rabbit AVN cells [33,41–44]. Accordingly, the effects of ET-1 on I_{Kr} were assessed by measurements of outward tail current amplitude at −40 mV, following 500 ms voltage commands to more positive potentials (between −30 and +50 mV). Figure 5A shows representative traces elicited following depolarisation to +30 mV in the absence and presence of ET-1, with the inset displaying the tails currents on a higher gain. ET-1 produced a 20–30% decrease in tail current amplitude. Figure 5B shows mean I–V relations for I_{Kr} tails in control and at steady-state in ET-1 (n = 5). Tail currents were significantly reduced at nearly all potentials between −20 and +50 mV. A fit to the data with equation 2 yielded activation $V_{0.5}$ values of −15.7±3.6 and −0.7±4.3 mV in control and ET-1 respectively ($p<0.05$; n = 5).

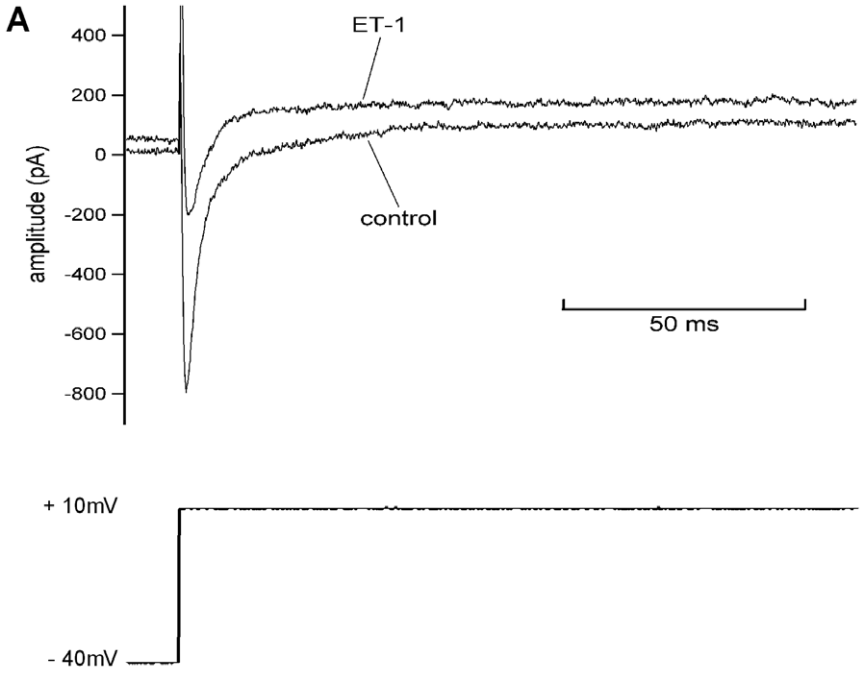

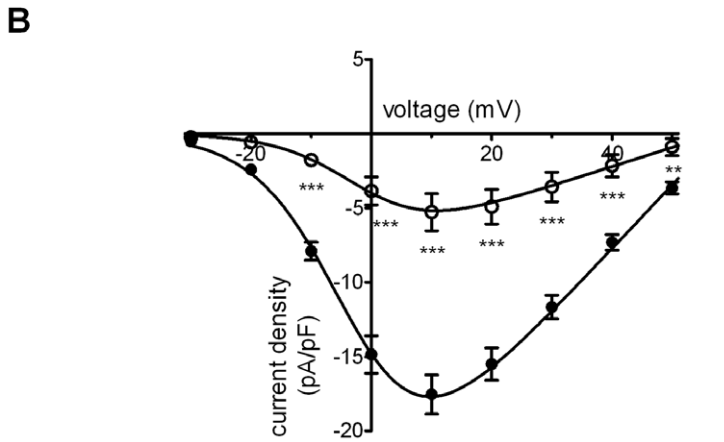

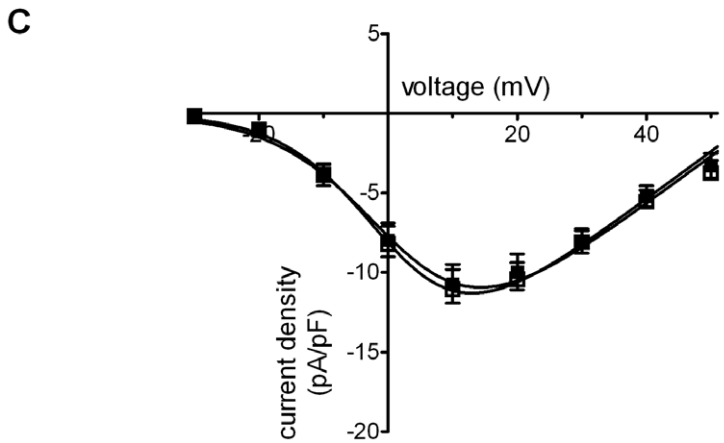

Figure 4. Effects of ET-1 on the L-type Ca^{2+} current ($I_{Ca,L}$). A. Representative records of $I_{Ca,L}$ (upper traces) elicited at +10 mV from a holding potential of −40 mV by protocol shown in lower traces, in both the absence (control) and presence of 10 nM ET-1. B. Plots of the mean I–V relations for $I_{Ca,L}$ (n = 11), measured as peak - end pulse difference current, in control (filled circles) and with ET-1 (open circles): I–V curves were fitted using

equation 1 (Methods) to give $V_{0.5}$ values of -2.7 ± 0.6 mV in control and -1.0 ± 1.9 mV in ET-1 ($p>0.1$). Corresponding k values were 7.1 ± 0.5 mV and 6.5 ± 1.7 mV in control and ET-1, respectively ($p>0.7$). C. I–V relations ($n=12$) for $I_{Ca,L}$ in the presence of 1 μM BQ-123 (filled squares) and when 10 nM ET-1 was applied in the maintained presence of BQ-123 (open squares). $V_{0.5}$ values were 2.1 ± 1.1 mV and 1.0 ± 1.0 mV respectively for BQ-123 and BQ-123+ET-1 ($p>0.4$), with corresponding k values of 8.2 ± 0.9 mV and 7.4 ± 0.9 mV ($p>0.5$). Asterisks in 'B' denote statistical significance ($p<0.01$ **, $p<0.001$ ***).
doi:10.1371/journal.pone.0033448.g004

Figure 5C shows mean tail current I–V relations for five experiments on cells exposed to BQ-123 prior to ET-1. There was no significant difference between BQ-123 alone and ET-1 in the presence of BQ-123 in tail current at any test voltage, implicating ET_A receptor activation in mediating the suppressive effect of ET-1 on I_{Kr} tail amplitude. Although ET-1 in the presence of BQ-123 still appeared to produce some right-ward shift in the fit to the current-voltage relationship ($V_{0.5}$ of -12.0 ± 5.1 mV in BQ-123 alone and -2.9 ± 6.4 mV in BQ-123 and ET-1; $n=5$), due to cell-to-cell variability in response the difference did not attain statistical significance ($p>0.3$). Similar to $I_{Ca,L}$ the effects of ET-1 on I_{Kr} did not reverse on ET-1 washout.

Investigation of the mechanism of AP quiescence

The rapid membrane potential hyperpolarisation with ET-1 during spontaneous AP recording shown in Figure 1 is consistent with the activation of an outward current over the diastolic membrane potential range. The ET-1 activated current observed here (Figures 2 and 3) exhibited a voltage dependence reminiscent of inwardly rectifying K^+ current in AVN cells activated by acetylcholine ($I_{K,ACh}$) or adenosine ($I_{K,Ado}$), each of which exert marked negative chronotropic effects on isolated AVN cells (e.g. [28,30]). Tertiapin/tertiapin-Q have been shown previously to inhibit sinoatrial $I_{K,ACh}$ (e.g. [45,46]) and to inhibit atrio-ventricular block induced in the guinea-pig by $I_{K,ACh}$ activation [47]. We hypothesised, therefore, that if ET-1 activates a current similar to $I_{K,ACh}$ in AVN cells, tertiapin-Q should prevent rapid ET-1 induced membrane potential hyperpolarisation and hyperpolarisation-associated cell quiescence. Consequently, experiments were performed in which tertiapin-Q was applied prior to ET-1 superfusion during spontaneous AP recording. Figure 6A shows representative results. Application of 300 nM tertiapin-Q alone did not alter spontaneous activity; however when ET-1 was subsequently applied in the maintained presence of tertiapin-Q, no rapid MDP hyperpolarisation or hyperpolarisation-associated quiescence was induced. Instead, there was a gradual depolarisation of MDP and decrease in AP amplitude (this cell depolarised and became quiescent within ~30 seconds of ET-1 in the presence of tertiapin-Q). Similar experiments were performed on seven spontaneously active cells; in none of them did ET-1 induce membrane potential hypolarisation in the presence of tertiapin-Q. Experiments were then performed to determine whether or not tertiapin-Q also inhibited ET-1 activated current under voltage clamp. Figure 6C shows that, in the presence of tertiapin-Q, ET-1 was unable to activate any inwardly rectifying instantaneous current. In a further 7 experiments, a second known inhibitor of inwardly rectifying ACh-activated K^+ conductances, Ba^{2+} ions, was applied (at 2 mM; [48]) during repetitive application of a descending voltage-ramp protocol. Ba^{2+} rapidly inhibited the ET-1 activated current in all cells tested (not shown). Collectively, the results of these experiments implicate ET-1 activation of an $I_{K,ACh}$-like current in the rapid suppression of spontaneous activity shown in Figure 1.

ET-1 effects on all currents observed under voltage-clamp were sensitive to ET_A receptor inhibition (Figures 2, 3, 4, and 5). Therefore, additional spontaneous AP recordings were performed in which the ET_A receptor inhibitor BQ-123 was applied prior to ET-1 superfusion. Figure 7 shows the results from one of six similar experiments. When ET-1 was applied following exposure of cells to BQ-123 no rapid membrane potential hyperpolarisation or suppression of spontaneous activity was observed. In a final set of experiments, the effects of a selective ET_B receptor agonist, IRL-1620 were investigated. IRL-1620 produced a small depolarisation of MDP (by 5.2 ± 1.4 mV; $n=5$) and decrease in AP overshoot (a mean reduction of 14.1 ± 1.4 mV; see Figure 8); however, no cell tested responded to IRL-1620 with membrane potential hyperpolarisation or quiescence. In contrast, when ET-1 was applied in the maintained presence of IRL-1620 it produced rapid membrane potential hyperpolarisation and quiescence (similar to that seen when ET-1 alone was applied; Figure 1).

Discussion

Placing novel findings in context

To our knowledge, the present data are the first to demonstrate directly modulation by ET-1 of AVN electrophysiology. Previously, intravenous administration of BQ-123 to anaesthetised pigs and, via intracoronary injection, to a small sample of human patients with coronary artery disease has been reported not to alter AV nodal conduction [49,50], suggestive of a lack of effect of basal endogeneous ET-1 on AV nodal conduction *via* ET_A receptors in those studies. On the other hand, intracoronary bolus injection of ET-1 to anesthetized dogs [26,27] and rats [26,27] has been shown to produce AV block, which is suggestive of an ability of increased ET-1 levels to modulate AVN electrical behaviour. The results of the present study show that ET-1 can suppress AVN cell activity, and the modulatory effects on AVN cellular electrophysiology seen here may help explain prior observations of ET-1 induced AV block [26,27]. This is also the first study to demonstrate tertiapin-Q sensitivity of an ET-1 activated K^+ current in any cell or tissue type. Several features of our findings merit more detailed discussion.

Comparison with previous studies

Whilst the effects of ET-1 on cardiac ion channel currents from other cardiac cell types have been widely studied, the most relevant data for comparison with the present study come from prior investigations of isolated *sinoatrial* node (SAN) cell and tissue preparations [21–23]. In 2001 Ono and colleagues demonstrated negative chronotropic effects of ET-1 on rabbit intact SAN preparations and isolated SAN cells [23]. Application of ET-1 at the same concentration used in the present study (10 nM) was able to induce quiescence in isolated SAN cells, which either did not readily reverse or reversed incompletely during the recording measurement period. However, the negative chronotropic effect of ET-1 seen in that study was accompanied by membrane potential hyperpolarisation only in some (rod-shaped) cells, whilst other (spindle-shaped) cells showed depolarisation of the MDP [23]. A separate study of rabbit SAN cells by Tanaka and colleagues produced results in good agreement with those in the present investigation: application of 10 nM ET-1 routinely led rapidly to cessation of spontaneous activity and to membrane potential hyperpolarisation [21]. In the present study, all spontaneously active AVN cells exposed to ET-1 exhibited rapid membrane

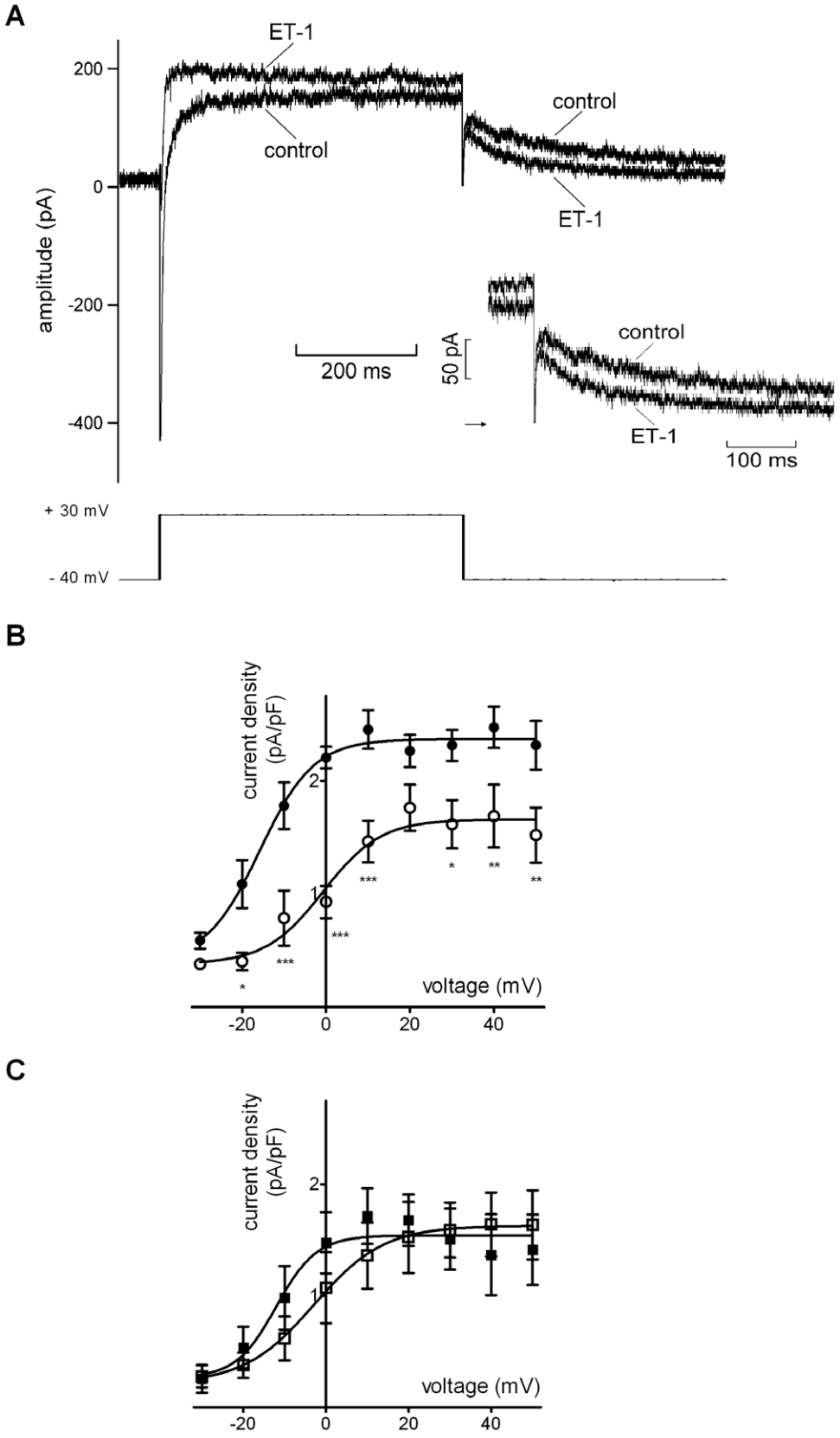

Figure 5. Effects of ET-1 on rapid delayed rectifier K^+ current tails. A. Upper traces show currents elicited on depolarisation to +30 mV and subsequent repolarization to −40 mV by protocol shown in lower trace. Deactivating tail currents on repolarization represent the I_{Kr} 'tail'. Currents are shown in control solution and in presence of 10 nM ET-1. Insert shows an expanded portion of the traces to highlight the 'tail' currents (the horizontal arrow in the inset denotes the zero current level). B. Mean 'tail' current I–V relationships for 5 cells, in absence (control, filled circles) and

presence (open circles) of 10 nM ET-1. I–V curves were fitted with equation 2 (Methods) to derive $V_{0.5}$ values of -15.7 ± 3.6 mV in control and -0.7 ± 4.3 mV in ET-1 ($p<0.05$), with respective k values of 6.4 ± 2.6 mV and 6.9 ± 3.9 mV ($p>0.9$). The 'tail' current was significantly reduced in presence of ET-1 at all voltages ranging from -20 to +50 mV except +20 mV. C. Mean I–V plots for I_{Kr} tails in the presence of 1 μM BQ-123 without (filled squares; n = 5) and with 10 nM ET-1 (open squares, n = 5 for all, except at +40 and +50 mV where n = 4). Derived $V_{0.5}$ values were -12.0 ± 5.1 mV and -2.9 ± 6.4 mV for BQ-123 and BQ-123+ET-1, respectively ($P>0.3$), with associated k values of 4.9 ± 4.4 and 8.4 ± 5.8 ($p>0.6$). Asterisks in B denote statistical significance ($p<0.05$ *, $p<0.01$ **, $p<0.001$ ***).
doi:10.1371/journal.pone.0033448.g005

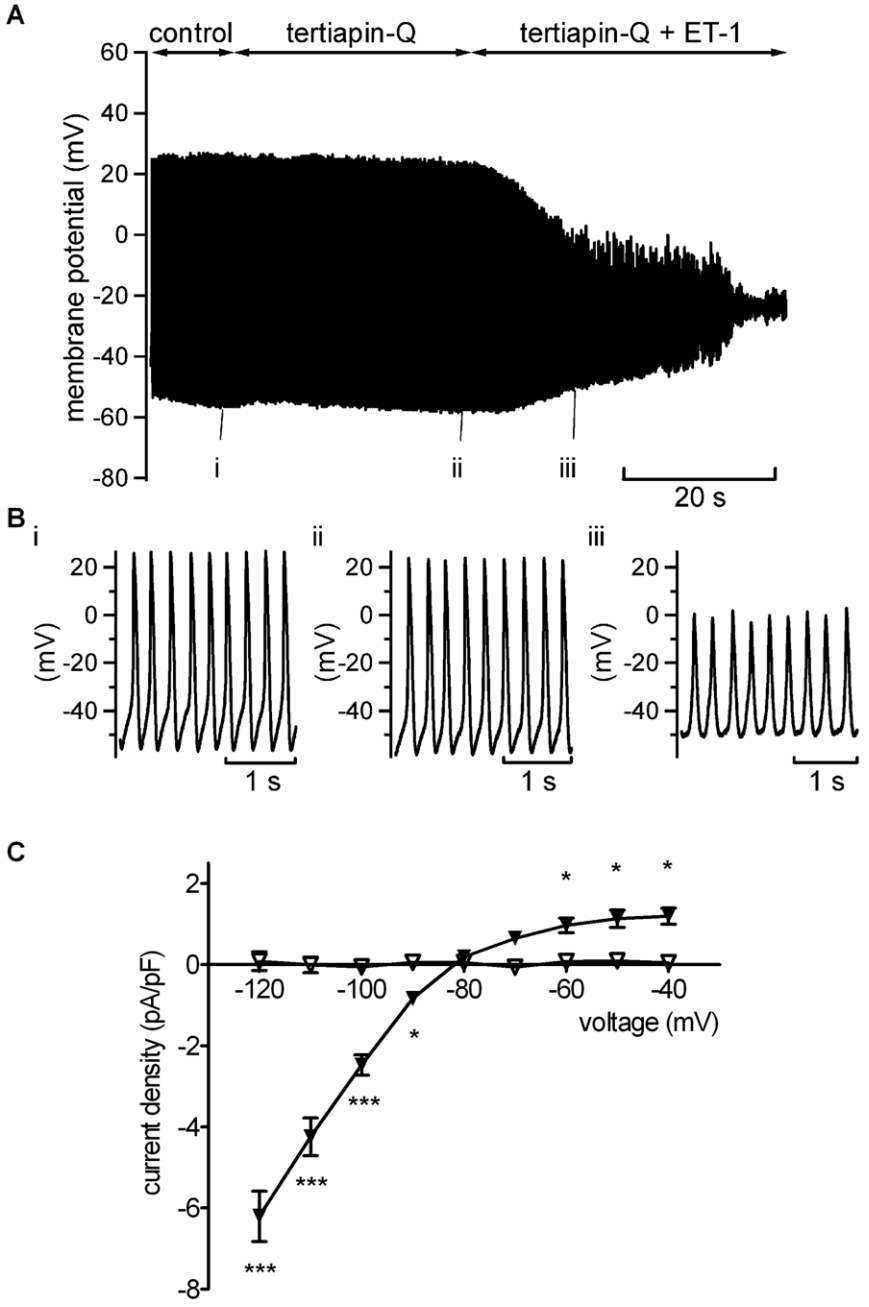

Figure 6. Effects of tertiapin-Q (TQ) on the effect of ET-1 on spontaneous APs and ET-1 activated current. A. Continuous recording of spontaneous activity in control, in the presence of TQ (300 nM) before and with application of 10 nM ET-1 in the maintained presence of TQ. Note the absence of immediate hyperpolarisation and cessation of APs evident in Figure 1. Bi, ii and iii show expanded records from recording in A, at time-points indicated: i taken during control, ii near the end of TQ alone and iii is taken at ~13 seconds of ET-1 application (at which time-point cells exposed to ET-1 alone had hyperpolarised and become quiescent). Similar results were obtained from 7 cells. C. Mean I–V relationships for the 10 nM ET-1 activated instantaneous current in absence (filled triangles, n = 14) and in presence of 300 nM TQ (open triangles, n = 7. except at −80 mV where n = 6). TQ prevented this action of ET-1. Asterisks in C denote statistical significance ($p<0.05$ *, $p<0.001$ ***).
doi:10.1371/journal.pone.0033448.g006

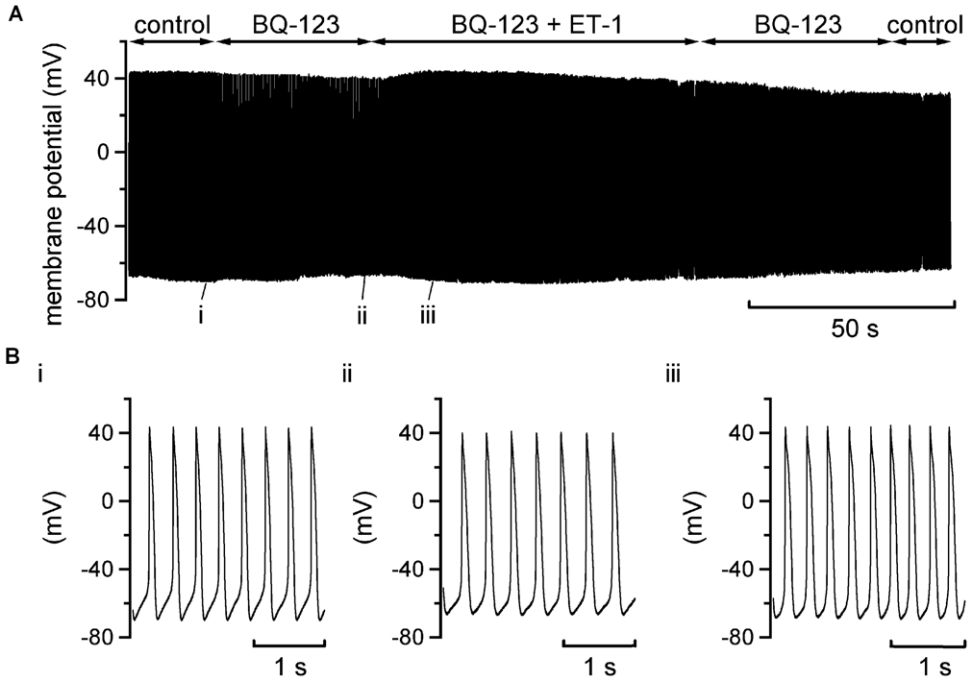

Figure 7. BQ-123 inhibition of the effects of ET-1 on spontaneous APs. A. Continuous recording of spontaneous activity in control solution, in presence of 1 μM BQ-123 before and during subsequent superfusion of 10 nM ET-1 in the maintained presence of BQ-123. BQ-123 prevented the ET-1 induced cessation of spontaneous APs and associated membrane potential hyperpolarisation. Bi, ii and iii show expanded extracts of the recording in A, at the time-points indicated: i taken during control, ii near the end of BQ-123 alone and iii is taken at ~13 seconds of ET-1 application in the presence of BQ-123 (at which time-point cells exposed to ET-1 alone had hyperpolarised and become quiescent). Similar results were obtained in 6 cells.
doi:10.1371/journal.pone.0033448.g007

potential hyperpolarisation and quiescence. Voltage-clamp data from both SAN studies indicated a marked inhibitory action of ET-1 on $I_{Ca,L}$ (~50% inhibition at 10 nM ET-1) [21,23] which is in reasonable agreement with our own observations for AVN cells. This contrasts with more modest effects of ET-1 on guinea-pig ventricular $I_{Ca,L}$ (~21% inhibition of basal $I_{Ca,L}$ by 20 nM ET-1 [51] and human ventricular $I_{Ca,L}$ (~33% inhibition of basal $I_{Ca,L}$ by 8 nM ET-1 [52]). Such differences may be accounted for by regional and/or species differences in ET-1 response, with rabbit primary and secondary pacemaker cell types exhibiting a greater response than ventricular myocytes from these two other species. The possibility of regional differences in response is supported by results from a study of rabbit ventricular myocytes [36] that reported weak bi-phasic effects of 10 nM ET-1 on basal $I_{Ca,L}$, with an inhibitory effect of smaller magnitude (~20%) than those seen for AVN (this study) or SAN [21,23]. Ono and colleagues also reported a modest reduction in delayed rectifier (I_K) tails across a wide range of voltages for spindle-shaped cells and up for voltages up to ~0 mV for rod-shaped cells, accompanied in both SAN types by positively shifted (~+5–+14 mV) I_K activation [23]. Tanaka and colleagues also showed suppression of SAN I_K by ET-1, though they did not study the voltage-dependence of the effect [21]. The activation $V_{0.5}$ values under control conditions for the tail currents investigated in this study are within the range reported previously for AVN I_{Kr} [33,41]. Although, in contrast with rabbit AVN cells that exhibit only I_{Kr} [33,41–44], both I_{Kr} and I_{Ks} have been seen in rabbit SAN cells [43,53], the activation characteristics of the current sensitive to ET-1 in the study of Ono and colleagues [23] are concordant with a primary identity as I_{Kr}. Both the present study and that of Ono and colleagues [23] report right-shifted current activation with ET-1, suggesting modification of a similar current in each case. Consequently, it is highly likely that, as reported previously for human ventricular I_{Kr} [52], ET-1 inhibits I_{Kr} from both secondary and primary pacemaker cell types.

Previously reported effects of ET-1 on I_f from SAN cells show some differences from those observed here for AVN myocytes. Thus, Ono and colleagues reported that 10 nM ET-1 activated I_f between ~−75 and −85 mV, but that it inhibited I_f at more negative voltages [23]; Tanaka and colleagues also reported an inhibitory action [22]. On the other hand, we saw significant augmentation of AVN cell I_f by ET-1, but only at potentials negative to the diastolic potential range. Similar to previous studies conducted under comparable recording conditions [29,33], I_f from AVN cells under control conditions here was small or absent over the diastolic potential range and the lack of any statistically significant effect of ET-1 at potentials positive to −100 mV makes it unlikely that modulation of I_f by ET-1 contributed significantly to effects seen under AP recording conditions. By contrast, the activation of an inwardly rectifying K^+ current, with significant ET-1 activated outward current between ~−40 and −80 mV is of central importance to the overall actions of ET-1 seen here. The ability of ET-1 to activate a current with similar properties to the muscarinic potassium current ($I_{K,ACh}$) was first demonstrated for non-pacemaker cardiac cells [54,55], although some studies have demonstrated an ability of ET-1 to inhibit $I_{K,ACh}$ and $I_{K,Ado}$ (e.g. [56–58]). Tanaka and colleagues demonstrated activation by ET-1 in rabbit SAN cells of an inwardly rectifying K^+ current similar to that seen here, also showing this to be Ba^{2+}-sensitive and to carry outward current over potentials relevant to the diastolic potential range [21]. Drici and colleagues have demonstrated that ACh-induced AV block in guinea-pig hearts is prevented by tertiapin at

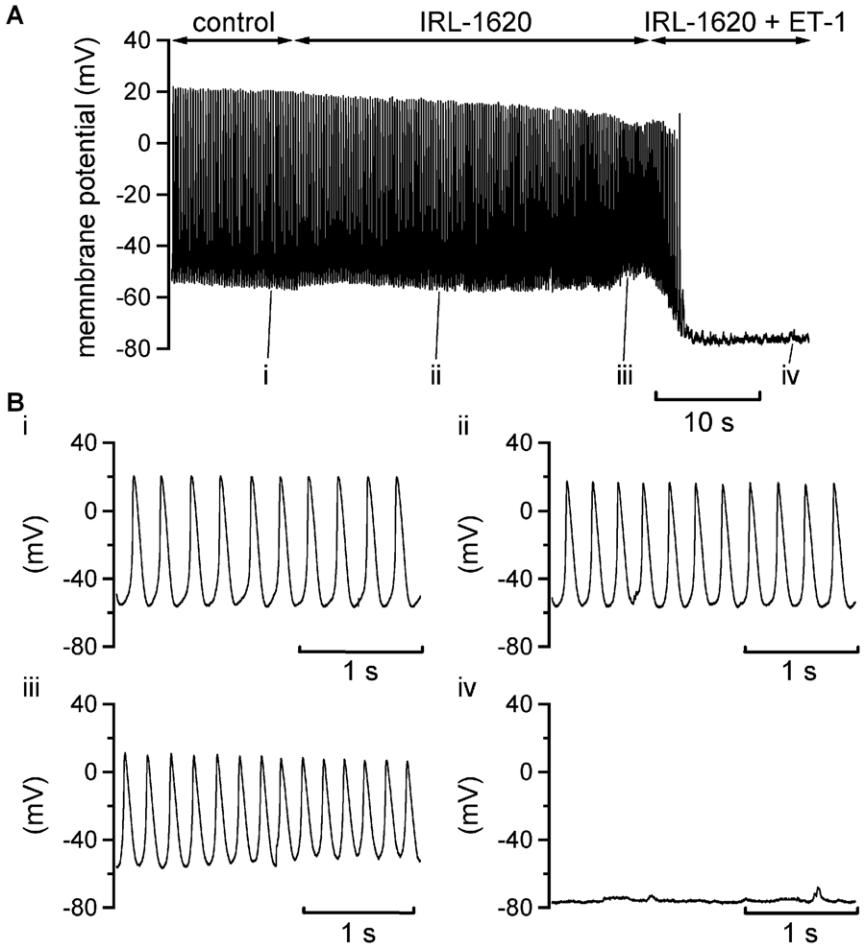

Figure 8. Effect of IRL-1620 on spontaneous APs. A. Slow time-base continuous recording of APs in control conditions, followed by the application of 300 nM IRL-1620 and following addition of 10 nM ET-1 in the maintained presence of IRL-1620. IRL-1620 did not abolish the spontaneous APs, whereas application of 10 nM ET-1 stopped spontaneous activity and hyperpolarized the membrane potential. Similar results were acquired in 5 cells. Bi, ii, iii and iv show expanded extracts of the recording shown in A, at the time-points indicated: i taken during control, ii and iii taken respectively mid-way and towards the end of IRL-1620 alone and iv is taken at ~13 seconds of ET-1 application in the presence of IRL-1620 (at which time-point cells exposed to ET-1 alone had hyperpolarised and become quiescent).
doi:10.1371/journal.pone.0033448.g008

concentrations including that used here, without non-selective effects of tertiapin on other important cardiac ionic currents [47]. Thus, the inhibition by tertiapin-Q of the ET-1 activated (Ba^{2+}-sensitive) inwardly rectifying current in AVN cells seen here identifies the underlying channels as similar to those that mediate $I_{K,ACh}$. It is also notable that activation of a similar K^+ current ($I_{K,Ado}$) contributes significantly to the known negative chronotropic and dromotropic effects of adenosine [30,59]. Moreover, it is evident from the complete lack of membrane potential hyperpolarisation when ET-1 was applied to cells treated with tertiapin-Q, that this current mediated the rapid hyperpolarisation and quiescence of AVN cells following ET-1 application. $I_{K,ACh}$ from the SAN has been shown to exhibit a time-dependent fade in the presence of continued muscarinic receptor activation as a result of desensitization [60,61] and our results indicate that a similar phenomenon occurs for ET-1 activated inwardly rectifying K^+ current in AVN cells. The mechanism underlying this effect remains to be elucidated and warrants future study. The progressive MDP depolarisation and decrease in AP amplitude seen when ET-1 was applied to tertiapin-Q treated cells can be explained, wholly or in part, by ET-1 inhibition of I_{Kr} (which would predispose towards membrane potential depolarisation) and of $I_{Ca,L}$ (which would decrease AP amplitude and may also offset AP prolongation anticipated with pure I_{Kr} inhibition), neither of which response showed time-dependent fade. Similarly, the persistence of an ET-1 effect following ET-1 washout, namely maintained quiescence and progressive membrane potential depolarisation (Figure 1), can be accounted for by continued ET-1 receptor activation following washout and by the peptide's effects on $I_{Kr}/I_{Ca,L}$ predominating as the inwardly rectifying current response became desensitized/faded. Our data in this regard are compatible with previously reported quasi-irreversible binding of ET-1 to cardiac myocytes ET (ET_A) receptors and on ET-receptor mediated signalling [39].

A central role for ET_A receptors

Autoradiographical examination of the human cardiac conduction system has demonstrated the presence of both ET_A and ET_B receptors in the AVN and atrio-ventricular conduction system [24], with a higher proportion of ET_B receptors and lower proportion of ET_A receptors in the AV conduction system than in the surrounding interventricular and interatrial septa [24]. mRNA for both ET

receptor types has been demonstrated to be widespread in the rabbit heart [23], with mRNA levels for ET_B in the SAN suggested to be similar to those in atria and ventricles, whilst those for ET_A have suggested to be lower [23]. Against this background, it is notable that effects of ET-1 on SAN action potentials and ionic currents have been reported to be highly sensitive to ET_A receptor blockade [21,23]. Inhibitory effects of ET-1 on SAN $I_{Ca,L}$ and I_K and the activation of $I_{K,ACh}$-like inward rectifier current were all abolished by selective ET_A blockade [21]. Our data provide strong evidence for a similar pivotal role for ET_A receptor involvement in ET-1 modulation of AVN cell activity, both at the level of effects on spontaneous APs and also for ionic currents. It is particularly notable that application of the ET_B-selective agonist IRL-1620 failed to replicate the rapid membrane potential hyperpolarisation and quiescence produced by ET-1 (and inhibited by BQ-123); whilst subsequent ET-1 application in the maintained presence of IRL-1620 led rapidly to these effects. This indicates that the dominant, rapid-onset effect of ET-1 under our conditions was activation of tertiapin-Q sensitive $I_{K,ACh}$-like current, mediated through ET_A receptors. Our data do not preclude entirely potential roles for ET_B receptor activation: application of IRL-1620 itself led to a modest reduction in AP magnitude and, under voltage-clamp, of $I_{Ca,L}$ (data not shown). Whether or not these actions of IRL-1620 are mediated through ET_B receptor activation *per se* or represent a non-selective action of this agent is unclear at this time. Efforts to pursue this line further through the use of a selective ET_B receptor antagonist, RES-701, were confounded by potential contaminating effects that led us to abandon its use. Nevertheless, what is very clear from our experiments is the dominant role played by ET_A receptor activation in the observed effects of ET-1, which is in good agreement with prior work on the SAN.

Limitations, future work and conclusions

Understanding of the cellular electrophysiology of the AVN and its modulation has tended to lag behind that of other cardiac regions, to a significant extent likely due to challenges inherent in isolating and working with single AVN cells. Accordingly, the present study is the first to characterise major actions of ET-1 on AVN APs and ionic currents and has identified a number of marked effects. However, whilst our voltage-clamp data can account for the principal effects of ET-1 seen on spontaneous AVN APs, this does not mean that the basis for all modulatory effects have yet been identified. For example, the underlying basis for the small amplitude spontaneous membrane potential oscillations in quiescent AVN cells following ET-1 treatment (Figure 1) remains to be elucidated. Recent data indicate that AVN activity is influenced by cellular Ca^{2+} cycling, likely through the interaction between Ca^{2+} released from internal stores and the sarcolemmal Na-Ca exchanger (NCX) [10,62,63]. ET-1 has been reported to stimulate NCX activity [64,65] and the effects of ET-1 on AVN NCX remain to be investigated. Additionally, it is well established that in atrial myocytes ET-receptor activation of IP_3 receptors can influence Ca^{2+} mobilization (e.g [66–68]) and IP_3 receptor activity has recently been proposed to modulate murine SAN activity [69]. Thus, potential additional effects of ET-1 on AVN activity mediated by the modulation of Ca^{2+} handling merits future enquiry. The experimental concentration of ET-1 used in this study (10 nM) lies within the range used in previous rabbit SAN and ventricular cardiomyocyte studies (1–100 nM; e.g. [21,23,36]) and is similar to that (8 nM) used to study ET-1 effects on undiseased human ventricular myocytes [52]. It should be noted that, whilst normal plasma levels of ET-1 are low (in the fM-pM range; e.g. [70,71]), considerably higher pericardial and tissue levels can be measured (e.g. [71,72]). We are not aware of data on endogenous ET-1 levels in AVN tissue *per se*, but a level of ~1.2 nM has been measured in rabbit left ventricle [71], whilst in human atrial tissue a mean level of ~19 nM (range ~2–64 nM) has been measured [72]. Thus, whilst the ET-1 concentration used in this (and other) studies is likely to exceed circulating plasma levels, it lies within measured cardiac tissue levels [71,72]. Additional avenues of future investigation opened by the present report include the determination of effects of wide-ranging ET-1 concentrations (cf [21]), the study of intracellular pathways mediating major identified effects, and investigation of effects of ET-1 on autonomic agonist modulation of AVN activity.

To summarise and conclude: the present study demonstrates for the first time that ET-1 activation of ET_A receptors produces a rapid suppression of spontaneous activity of rabbit AVN cells. ET-1 also inhibits both I_{Kr} and $I_{Ca,L}$ from AVN cells whilst activating K^+ current through channels identical to those responsible for muscarinic inwardly rectifying K^+ current. This current mediates the initial rapid hyperpolarisation and quiescence produced by ET-1, whilst I_{Kr} and $I_{Ca,L}$ suppression are likely to contribute to maintained suppression of excitability. Bolus injection of ET-1 in previous experimental studies on anaesthetised animals [26,27] is likely to have produced a rapid, local rise in ET-1 in blood perfusing the AVN. Rapid membrane potential hyperpolarisation through activation of an $I_{K,ACh}$-like current and suppression of currents important to AVN AP genesis can account for the AV block subsequently observed in those studies [26,27] - a proposition that can be tested further through future targeted experiments using intact AVN preparations.

Acknowledgments

The authors thank Mrs Lesley Arberry for technical assistance, Dr Palash Barman and Ms Hanne Gadeberg for help with cell isolation, Prof Clive Orchard for valuable discussion and encouragement, and Dr Antony Workman (Glasgow) for valuable discussion.

Author Contributions

Conceived and designed the experiments: JCH AFJ SCMC. Performed the experiments: SCMC HWC. Analyzed the data: SCMC HWC. Wrote the paper: JCH AFJ SCMC. Involved in original design of the study and edited/commented on a completed form of the manuscript: GLS.

References

1. Tawara S (1906) Das Reizleitungssystem des Saugetierherzens. 1 ed. Jena, Germany: Fischer.
2. Meijler FL, Janse MJ (1988) Morphology and electrophysiology of the mammalian atrioventricular node. Physiol Rev 68: 608–47.
3. Anderson RH, Janse MJ, van Capelle FJL, Bilette J, Becker AE, et al. (1974) A combined morphological and electrophysiological study of the atrioventricular node of the rabbit heart. Circ Res 35: 909–922.
4. Langendorf R, Pick A (1956) Concealed conduction. Further evaluation of a fundamental aspect of propagation of the cardiac impulse. Circulation 13: 381–399.
5. Childers R (1977) The AV node: Normal and abnormal physiology. Progress in Cardiovascular Diseases XIX(5): 361–81.
6. Hancox JC, Yuill KH, Mitcheson JS, Convery MK (2003) Progress and gaps in understanding the electrophysiological properties of morphologically normal cells from the cardiac atrioventricular node. International Journal of Bifurcation and Chaos 13: 3675–3691.
7. Efimov IR, Nikolski VP, Rothenberg F, Greener ID, Li J, et al. (2004) Structure-function relationship in the AV junction. Anat Rec A Discov Mol Cell Evol Biol 280: 952–965.
8. Mangoni ME, Nargeot J (2008) Genesis and regulation of the heart automaticity. Physiol Rev 88: 919–982.
9. Inada S, Hancox JC, Zhang H, Boyett MR (2009) One-dimensional mathematical model of the atrioventricular node including atrio-nodal, nodal, and nodal-his cells. Biophys J 97: 2117–2127.

10. Cheng H, Smith GL, Hancox JC, Orchard CH (2011) Inhibition of spontaneous activity of rabbit atrioventricular node cells by KB-R7943 and inhibitors of sarcoplasmic reticulum Ca^{2+} ATPase. Cell Calcium 49: 56–65.
11. Rubanyi GM, Polokoff MA (1994) Endothelins: molecular biology, biochemistry, pharmacology and pathophysiology. Pharmac Rev 46: 325–415.
12. Russell FD, Molenaar P (2000) The human endothelin system: ET-1 synthesis, storage, release and effect. TIPS 21: 353–359.
13. Mebazaa A, Mayoux E, Maeda K, Martin LD, Lakatta EG, et al. (1993) Paracrine effects of endocardial endothelial cells on myocyte contraction mediated via endothelin. Am J Physiol 265: H1841–1846.
14. MacCarthy PA, Grocott-Mason R, Prendergast BD, Shah AM (2000) Contrasting inotropic effects of endogenous endothelin in the normal and failing human heart: studies with an intracoronary ET(A) receptor antagonist. Circulation 101: 142–147.
15. Wenzel RR, Fleisch M, Shaw S, Noll G, Kaufmann U, et al. (1998) Hemodynamic and coronary effects of the endothelin antagonist Bosentan in patients with coronary artery disease. Circulation 98: 2235–2240.
16. Sutsch G, Bertel O, Kiowski W (1997) Acute and short-term effects of the nonpeptide endothelin-1 receptor antagonist Bosentan in humans. Cardiovasc Drugs Ther 10: 717–725.
17. Duru F, Barton M, Luscher TF, Candinas R (2001) Endothelin and cardiac arrhythmias: do endothelin antagonists have a therapeutic potential as antiarrhythmic drugs? Cardiovasc Res 49: 272–280.
18. Kawanabe Y, Nauli SM (2011) Endothelin. Cell Mol Life Sci 68: 195–203.
19. Wainwright CL, McCabe C, Kane KA (2005) Endothelin and the ischaemic heart. Curr Vasc Pharmacol 3: 333–341.
20. Kaski JC, Elliot PM, Salomone O, Dickinson K, Gordon D, et al. (1995) Concentration of circulating plasma endothelin in patients with angina and normal coronary angiograms. Br Heart J 74: 620–624.
21. Tanaka H, Habuchi Y, Yamamoto T, Nishio M, Morikawa J, et al. (1997) Negative chronotropic actions of endothelin-1 on rabbit sinoatrial node pacemaker cells. Br J Pharmacol 122: 321–329.
22. Tanaka H, Habuchi Y, Nishio M, Yamamoto T, Suto F, et al. (1998) Endothelin-1 inhibits pacemaker currents in rabbit SA nodal cells. J Cardiovasc Pharmacol 31(S1): S440–S442.
23. Ono K, Masumiya H, Sakamoto A, Christe G, Shijuku T, et al. (2001) Electrophysiological analysis of the negtive chronotropic effect of endothelin-1 in rabbit sinoatrial node cells. J Physiol 537: 467–488.
24. Molenaar P, O'Reilly G, Sharkey A, Kuk RE, Harding DP, et al. (1993) Characterization and localization of endothelin receptor sub-types in the human atrioventricular conducting system and myocardium. Circ Res 72: 526–538.
25. Yamasaki H, Niwa M, Yamashita K, Katoka Y, Shigematsu K, et al. (1989) Specific 125I-endothelin-1 binding sites in the atrioventricular node of the porcine heart. Eur J Pharmacol 168: 247–250.
26. Muramatsu K, Tomoike H, Ohara Y, Egashira S, Nakamura M (1991) Effects of endothelin-1 on epicardial coronary tone, coronary blood flow, ECG-ST change and regional wall motion in anesthetized dogs. Heart and Vessels 6: 191–196.
27. Harada K, Miwa A, Kaneta S, Izawa T, Fukushima H, et al. (1993) Effects of KRN2391, nicorandil and diltiazem on the changes in the electrocardiogram caused by endothelin-1 in anaesthetized rats. Br J Pharmacol 109: 679–684.
28. Hancox JC, Levi AJ, Lee CO, Heap P (1993) A method for isolating rabbit atrioventricular node myocytes which retain normal morphology and function. Am J Physiol 265: H755–H766.
29. Hancox JC, Levi AJ (1994) The hyperpolarisation-activated current, I_f, is not required for pacemaking in single cells from the rabbit atrioventricular node. Pflugers Arch 427: 121–128.
30. Martynyuk AE, Kane KA, Cobbe SM, Rankin AC (1995) Adenosine increases potassium conductance in isolated rabbit atrioventricular nodal myocytes. Cardiovas Res 30: 668–675.
31. Munk AA, Adjeiman RA, Zhao J, Ogbaghebriel A, Shrier A (1996) Electrophysiological properties of morphologically distinct cells isolated from the rabbit atrioventricular node. J Physiol 493: 801–818.
32. Ren FX, Niu XL, Ou Y, Han ZH, Ling FD, et al. (2006) Morphological and electrophysiological properties of single myocardial cells from Koch triangle of rabbit heart. Chin Med J (Engl) 119: 2075–2084.
33. Cheng H, Smith GL, Orchard CH, Hancox JC (2009) Acidosis inhibits spontaneous activity and membrane currents in myocytes isolated from the rabbit atrioventricular node. J Mol Cell Cardiol 46: 75–85.
34. Isenberg G, Klockner U (1982) Calcium tolerant ventricular myocytes prepared by incubation in a ''KB medium''. Pflugers Arch 395: 6–18.
35. Levi AJ, Hancox JC, Howarth FC, Croker J, Vinnicombe J (1996) A method for making rapid changes of superfusate whilst maintaining temperature at 37°C. Pflugers Arch 432: 930–937.
36. Watanabe T, Endoh M (1999) Characterization of the endothelin-1 induced regulation of L-type Ca^{2+} current in rabbit ventricular myocytes. Naunyn-Schmiedeberg's Arch Pharmacol 360: 654–664.
37. Ihara M, Noguchi K, Saeki T, Fukuroda T, Tsuchida S, et al. (1992) Biological profiles of highly potent novel endothelin antagonists selective for the ET_A receptor. Life Sci 50: 247–255.
38. Takai M, Umemura I, Yamasaki K, Watakabe T, Fujitani Y, et al. (1992) A potent and specific agonist, Suc-[Glu9,Ala11,15]-endothelin-1(8–21), IRL 1620, for the ET_B receptor. Biochem Biophys Res Commun 184: 953–959.
39. Hilal-Dandan R, Villegas S, Gonzalez A, Brunton LL (1997) The quasi-irreversible nature of endothelin binding and G protein-linked signaling in cardiac myocytes. J Pharmacol Exp Ther 281: 267–273.
40. Mitcheson JS, Hancox JC (1997) Modulation by mexiletine of action potentials, L-type Ca current and delayed rectifier K current recorded from isolated rabbit atrioventricular nodal myocytes. Pflugers Arch 434: 855–858.
41. Mitcheson JS, Hancox JC (1999) An investigation of the role played by the E-4031-sensitive (rapid delayed rectifier) potassium current in isolated rabbit atrioventricular nodal and ventricular myocytes. Pflugers Arch 438: 843–850.
42. Sato N, Tanaka H, Habuchi Y, Giles WR (2000) Electrophysiological effects of ibutilide on the delayed rectifier K^+ current in rabbit sinoatrial and atrioventricular node cells. Eur J Pharmacol 404: 281–288.
43. Habuchi Y, Han X, Giles WR (1995) Comparison of the hyperpolarisation-activated and delayed rectifier currents in rabbit atrioventricular node and sinoatrial node. Heart and Vessels S9: 203–6.
44. Howarth FC, Levi AJ, Hancox JC (1996) Characteristics of the delayed rectifier potassium current (I_K) compared in myocytes isolated from the atrioventricular node and ventricule of the rabbit heart. Pflugers Arch 431: 713–22.
45. Bolter CP, English DJ (2008) The effects of tertiapin-Q on responses of the sinoatrial pacemaker of the guinea-pig heart to vagal nerve stimulation and muscarinic agonists. Exp Physiol 93: 53–63.
46. Yamada M (2002) The role of muscarinic K^+ channels in the negative chronotropic effect of a muscarinic agonist. J Pharmacol Exp Ther 300: 681–687.
47. Drici MD, Diochot S, Terrenoire C, Romey G, Lazdunski M (2000) The bee venom tertiapin underlines the role of I_{KACh} in acetylcholine-induced atrioventricular blocks. Br J Pharmacol 131: 569–577.
48. Yang ZK, Boyett MR, Janvier NC, McMorn SO, Shui Z, et al. (1996) Regional differences in the negative inotropic effect of acetylcholine within the canine ventricle. J Physiol 492: 789–806.
49. Gelzer AR, Attmann T, Radicke D, Nydam D, Candinas R, et al. (2004) Effects of acute systemic endothelin receptor blockade on cardiac electrophysiology in vivo. J Cardiovasc Pharmacol 44: 564–570.
50. Kolettis TM, Kyriakides ZS, Leftheriotis D, Papalambrou A, Kremastinos DT, et al. (2003) Electrophysiologic effects of endothelin receptor-A blockade in patients with coronary artery disease. J Interv Card Electrophysiol 8: 173–179.
51. Xie LH, Horie M, James AF, Watanuki M, Sasayama S (1996) Endothelin-1 inhibits L-type Ca currents enhanced by isoproterenol in guinea-pig ventricular myocytes. Pflugers Arch 431: 533–539.
52. Magyar J, Iost N, Kortvely A, Banyasz T, Virag L, et al. (2000) Effects of endothelin-1 on calcium and potassium currents in undiseased human ventricular myocytes. Pflugers Arch 441: 144–149.
53. Lei M, Cooper PJ, Camelliti P, Kohl P (2002) Role of the 293B-sensitive, slowly activating delayed rectifier potassium current, I_{Ks}, in pacemaker activity of rabbit isolated sino-atrial node cells. Cardiovasc Res 53: 68–79.
54. Kim D (1991) Endothelin activation of an inwardly rectifying K^+ current in atrial cells. Circ Res 69: 250–255.
55. Ono K, Tsujimoto G, Sakamoto A, Eto K, Masaki T, et al. (1994) Endothelin-A receptor mediates cardiac inhibition by regulating calcium and potassium currents. Nature 370: 301–304.
56. Spiers JP, Kelso EJ, McDermott BJ, Scholfield CN, Silke B (1996) Endothelin-1 mediated inhibition of the acetylcholine-activated potassium current from rabbit isolated atrial cardiomyocytes. Br J Pharmacol 119: 1427–1437.
57. Cho H, Lee D, Lee SH, Ho W-K (2005) Receptor-induced depletion of phosphatidylinositol 4,5-bisphosphate inhibits inwardly rectifying K^+ channels in a receptor-specific manner. Proc Natl Acad Sci U S A 102: 4643–4648.
58. Cho H (2010) Regulation of adenosine-activated GIRK channels by Gq-coupled receptors in mouse atrial myocytes. Korean J Physiol Pharmacol 14: 145–150.
59. Rankin AC, Martynyuk AE, Workman AJ, Kane KA (1997) Ionic mechanisms of the effect of adenosine on single rabbit atrioventricular node myocytes. Can J Cardiol 13: 1183–1187.
60. Boyett MR, Roberts A (1987) The fade in response to acetylcholine at the rabbit isolated sinoatrial node. J Physiol 393: 171–194.
61. Honjo H, Kodama I, Zang WJ, Boyett MR (1992) Desensitization to acetylcholine in single sinoatrial node cells isolated from rabbit hearts. Am J Physiol 263: H1779–89.
62. Nikmaram MR, Liu J, Abdelrahman M, Dobrzynski H, Boyett MR, et al. (2008) Characterization of the effects of ryanodine, TTX, E-4031 and 4-AP on the sinoatrial and atrioventricular nodes. Prog Biophys Mol Biol 96: 452–464.
63. Ridley JM, Cheng H, Harrison OJ, Jones SK, Smith GL, et al. (2008) Spontaneous frequency of rabbit atrioventricular node myocytes depends on SR function. Cell Calcium 44: 580–591.
64. Ballard C, Schaffer S (1996) Stimulation of the Na^+/Ca^{2+} exchanger by phenylephrine, angiotensin II and endothelin 1. J Mol Cell Cardiol 28: 11–17.
65. Zhang YH, James AF, Hancox JC (2001) Regulation by endothelin-1 of Na^+-Ca^{2+} exchange current (I_{NaCa}) from guinea-pig isolated ventricular myocytes. Cell Calcium 30: 351–360.
66. Mackenzie L, Roderick HL, Proven A, Conway SJ, Bootman MD (2004) Inositol 1,4,5-trisphosphate receptors in the heart. Biol Res 37: 553–557.
67. Mackenzie L, Bootman MD, Laine M, Berridge MJ, Thuring J, et al. (2002) The role of inositol 1,4,5-trisphosphate receptors in Ca^{2+} signalling and the generation of arrhythmias in rat atrial myocytes. J Physiol 541: 395–409.

68. Mackenzie L, Roderick HL, Berridge MJ, Conway SJ, Bootman MD (2004) The spatial pattern of atrial cardiomyocyte calcium signalling modulates contraction. J Cell Sci 117: 6327–6337.
69. Ju YK, Liu J, Lee BH, Lai D, Woodcock EA, et al. (2011) Distribution and functional role of inositol 1,4,5-trisphosphate receptors in mouse sinoatrial node. Circ Res 109: 848–857.
70. Mitani H, Takimoto M, Bandoh T, Kimura M (2000) Increases in vascular endothelin-converting enzyme activity and endothelin-1 level on atherosclerotic lesions in hyperlipedimic rabbits. Eur J Pharmacol 387: 313–319.
71. Loffler B-M, Roux S, Kalina B, Clozel M, Clozel J-P (1993) Influence of congestive heart failure on endothelin levels and receptors in rabbits. J Mol Cell Cardiol 24: 407–416.
72. Horkay F, Laine M, Szokodi I, Leppaluoto J, Vuolteenaho O, et al. (1995) Human pericardial fluid contains the highest amount of endothelin-1 of all mammalian biologic fluids thus far tested. J Cardiovasc Pharmacol 26: S502–S504.